

Effect of Concentrations of Lead Acetate on Structural, Optical and Electrical Properties of Chemically Deposited Nanostructured Films of PbS

Bhaskarjyoti Baruah¹ and Kanak Ch. Sarma²

¹Dept. Of Physics, D. R. College, Golaghat, Assam, India-785621

²Dept. of Instrumentation and USIC, Gauhati University Guwahati, Assam, India -781014

E-mail: ¹bhaskar.drc@gmail.com, ²kanak_sarma50@rediffmail.com

Abstract—Thin films of PbS on glass substrates have been prepared by CBD method with lead acetate as the Pb source and thiourea as S source at pH=12. The concentration of lead acetate has been varied from 0.5M to 1.2M at the step of 0.1M. We observed that the crystallite size decreases from 37.43 nm to 19.17 nm and strain increases as the concentration of lead acetate increases from 0.5M to 1.2M. The quantum confinement in the films are evident as the optical band gap increased from 1.4 eV at 0.5M to 2.7 eV at 1.2M. The widths of the midgap states have been signified by the Urbach energy which assumed different values at different molarities. Another effect of this change of concentration of lead acetate is to decrease the electrical conductivity of the films from $1.87 \times 10^{-3} (\Omega\text{cm})^{-1}$ at 0.5M to $6 \times 10^{-5} (\Omega\text{cm})^{-1}$ at 1.2M.

1. INTRODUCTION

PbS, characterized by narrow band gap of 0.41 eV [1] and large excitonic Bohr radius of 18 nm [2], is considered to be a good candidate for band gap tuning and finds many applications in optoelectronics [3-7]. For deposition of PbS thin film, Chemical Bath Deposition (CBD) method is widely used owing to its simplicity and cost effectiveness. The properties of the films deposited by CBD are sensitive to various deposition parameters such as complexing agent [8], pH [9], deposition temperatures [10], substrates [11] etc. In the CBD of PbS, a number of researchers have reported the concentration of Pb source or S source as another important parameter. For example, Seghaier et.al [12] experimentally determined the optimum concentration of lead nitrate and thiourea for obtaining a well crystalline film. Choudhury et.al [13] demonstrated that the structural and optical properties of the films are sensitive to the lead precursor solution. Zaman et.al [14] reported change of band gap and shift of carrier type with the concentration of Pb source. Thiagarajan et.al [15] observed the grain size and absorbance to increase at higher precursor concentrations. Beddek et.al [16] and Preetha et.al [17] demonstrated that the properties of the films are not only influenced by the concentrations of precursors but also their nature as well.

Although above researchers studied the effect of concentrations of Pb source and/or S source on various properties of the PbS film, they fixed other parameters at their chosen value which are also important as far as the properties of the films are concerned. In this work, we chose a different set of reaction parameters and analysed the effect of concentration of Pb source (lead acetate) on structural, optical and electrical properties of nanostructured PbS thin film prepared by CBD method to observe how grain size, strain, band gap and electrical conductivity follow pattern of change with the concentration of lead acetate.

2. EXPERIMENTAL DETAILS

Solutions of $\text{Pb}(\text{CH}_3\text{COO})_2 \cdot 3\text{H}_2\text{O}$ of concentrations 0.5M, 0.6M, 0.7M, 0.8M, 0.9M, 1.0M, 1.1M and 1.2M have been prepared in bidistilled water. To 5 ml of each solution, 2ml. of 1M triethanolamine (TEA) was added and stirred. Then 2M NaOH was added until the pH becomes 11. After addition of NaOH, initially white precipitate was observed which redissolved on further addition of NaOH. After inserting the chemically and ultrasonically cleaned glass substrates, 6 ml of 1M thiourea was added and the bath was topped up with distilled water in order to make the total volume of 100 ml. Within five minutes, the colour of the baths changed to black. After two hours of deposition at 60°C (constant temperature maintained with the help of water bath), the films were taken out of the baths, washed with doubly distilled water, dried and stored in vacuum desiccator with silica gel. The sides of the substrates facing the wall of the beaker were retained for characterization and the other sides were removed with the help of a dilute acid. The films were coded as 0.5M, 0.6M, 0.7M, 0.8M, 0.9M, 1.0M, 1.1M and 1.2M respectively depending upon the concentration of lead acetate used for the deposition of the films. All the reagents were of AR grade.

The pH was measured by Eutech pH700 digital meter. The X-ray diffraction pattern of the films were recorded by Bruker AXS D8 Advance diffractometer at room temperature with

CuK α radiation having wavelength 1.5406Å and Si(Li) PSD detector operated at 40 kV and 35 mA. The energy dispersive X-ray analysis (EDAX) were studied by Jeol JSM-6390 scanning electron microscope. The optical absorption and transmission were measured by Hitachi U-3900 UV-Vis spectrophotometer. The current-voltage characteristics were recorded by Keithley 2400 Electrometer using gap type silver electrodes.

3. RESULTS AND DISCUSSIONS

3.1. Structural Properties by XRD:

The X ray diffraction (XRD) pattern of the films are shown in the fig 1. Comparison with ICDD Card no. 78-1900 confirms that the XRD peaks correspond to PbS having fcc structure. The 0.5M film is highly (200) oriented ($I_{200}/I_{111}=6.39$) but as the molarity of the $Pb(CH_3COO)_2 \cdot 3H_2O$ increases, the intensity of the (111) peak increases relative to the (200) peak (Table 1). When the molarity of $Pb(CH_3COO)_2 \cdot 3H_2O$ becomes 1.2M, the film deposited has (111) plane as the most preferred orientation. As evident from the XRD pattern, the 0.5M film is highly crystalline and the crystallinity deteriorates at higher molarity.

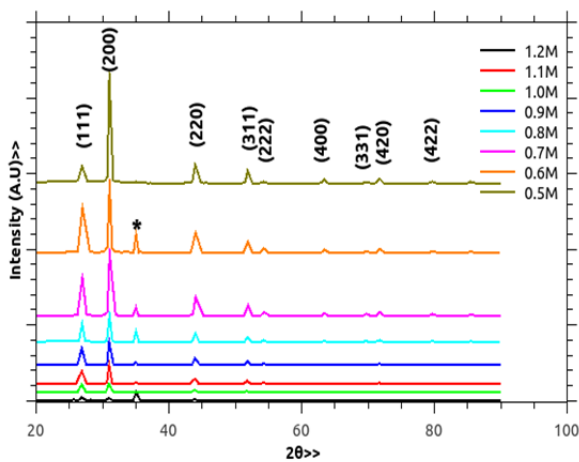


Fig. 1: XRD pattern of the films

Table 1: Structural, optical and electrical parameters of the films

[Pb(CH ₃ COO) ₂ ·3H ₂ O] (mol)	a(Å)	D (nm)	$\epsilon(x10^{-3})$	E_g (eV)	E_u (eV)	σ (Ωcm) ⁻¹
0.5	5.922	37.43	3.61	1.4	0.51	1.88×10^{-3}
0.6	5.93	27.86	4.85	1.4	0.99	3.36×10^{-3}
0.7	5.929	28.5	4.74	1.9	1.14	1.65×10^{-3}
0.8	5.932	25.7	5.26	1.9	0.58	3.31×10^{-4}
0.9	5.933	28.41	4.76	1.7	0.69	-----
1.0	5.913	23.07	5.87	2.5	0.90	10^{-4}
1.1	5.933	27.15	4.98	2.3	0.77	-----
1.2	5.893	19.17	7.07	2.7	0.92	6×10^{-5}

[Pb(CH₃COO)₂·3H₂O]=Concentration of Pb(CH₃COO)₂·3H₂O; a=Lattice Constant; ϵ = strain; D=Crystallite Size; E_g =Direct Band Gap; E_u =Urbach Energy; σ = Conductivity

As evident from the XRD pattern, the 0.5M film is highly crystalline and the crystallinity deteriorates at higher molarity.

The crystallite sizes as calculated from the Debye-Scherrer formula, comes out 37.43 nm for 0.5M film and decreases as the molarity of $Pb(CH_3COO)_2 \cdot 3H_2O$ increases. The least crystallite size (19.17 nm) was obtained for 1.2M. The crystallite sizes for all the concentrations of $Pb(CH_3COO)_2 \cdot 3H_2O$ are recorded in Table 3.2.

The systematic error free values of lattice constant (a), determined from the Nelson- Riley equation [18] are reported in the Table 1. It is observed from the table that there exists notable deviations of lattice constants of 1M and 1.2M films from the strain free bulk value of 5.929Å (card no. 78-1900) implying that these two films are highly strained in comparison to the remaining films.

The strain (ϵ) as calculated from the formula [19]

$$\epsilon = \beta \cot\theta/4 \tag{1}$$

(where β is the fwhm at the angle of diffraction 2θ) are the least when the concentration of $Pb(CH_3COO)_2 \cdot 3H_2O$ is 0.5M and the highest at $Pb(CH_3COO)_2 \cdot 3H_2O$ concentration of 1M and 1.2M. This is expected as the deviation of lattice constants of these two films from the strain free values were recorded to be the most prominent. Because of smaller crystallite sizes, the grain boundary densities are maximum in these two films leading to maximum strain.

An additional peak at $2\theta \sim 34.8^\circ$ marked * appears in all the films except 0.5M. This peak may correspond to some impurity phase resulting from nonstoichiometry or oxidation of the films. The EDAX give the Pb/S elemental ratio as 1.04, 2.98 and 0.85 for 0.5M, 1.0M and 1.2M respectively. That is, the 0.5M film is stoichiometric but not the other two. This leads us to believe that as the concentration of $Pb(CH_3COO)_2 \cdot 3H_2O$ deviates from 0.5M, the films become nonstoichiometric. This nonstoichiometric formation may give either Pb rich or S rich films which causes the additional peak to appear in the XRD pattern [20, ICDD PDF Card No.:00-020-1225]. Detection of oxygen atoms in the EDAX spectra also suggests the possibility of formation of $PbSO_4$ by the oxidation of PbS as this XRD peak may correspond to the (301) plane of $PbSO_4$ [12].

One possible explanation of the above observations regarding variation of crystallite size and microstrain may be that at 0.5M concentration of $Pb(CH_3COO)_2 \cdot 3H_2O$, the Pb^{2+} ions are released from the complexed bound state in very controlled manner and the nucleation and growth

at the substrate proceeds in such a rate that is suitable for growth of well crystalline stoichiometric film. On the other hand, at larger concentrations of $\text{Pb}(\text{CH}_3\text{COO})_2 \cdot 3\text{H}_2\text{O}$, the reaction rate becomes high owing to larger concentrations of Pb^{2+} s which in turn makes the nucleation rate higher leading to smaller crystallites with high microstrain.

3.2. Optical Properties of the films

The variation of optical absorbance(A) and transmittance(T) of the films against wavelength are shown in the fig. 2[(a)-(b)] in the wavelength range of 300-800 nm. It is observed that the films prepared at $[\text{Pb}(\text{CH}_3\text{COO})_2 \cdot 3\text{H}_2\text{O}] = 0.5\text{-}0.7\text{M}$ shows high absorbance in the visible region with least transmittance. It may be due to the superior crystallinity of these films as evidenced by the XRD spectra. The 1.2M film shows maximum transmittance This is the film whose crystallinity is the least with the least grain size and the highest microstrain.

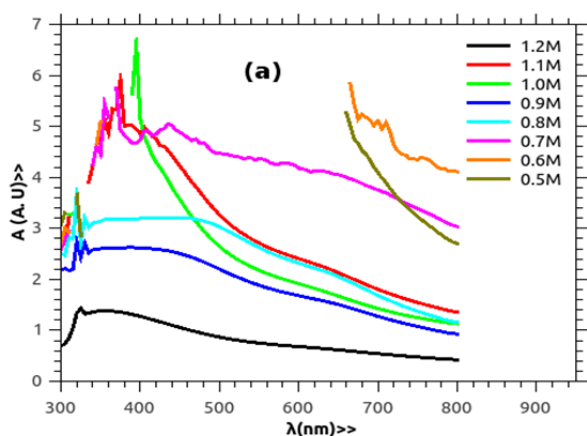


Fig. 2: Optical (a) absorbance and (b) transmittance of the films plotted against wavelength of incident light

The direct band gap of the films [21] were obtained in the range of 1.4-2.7 eV at various molarities of $\text{Pb}(\text{CH}_3\text{COO})_2 \cdot 3\text{H}_2\text{O}$ (Fig.3 and Table 1). This is a marked blue shift from the bulk value of 0.41 eV indicating quantum confinement.

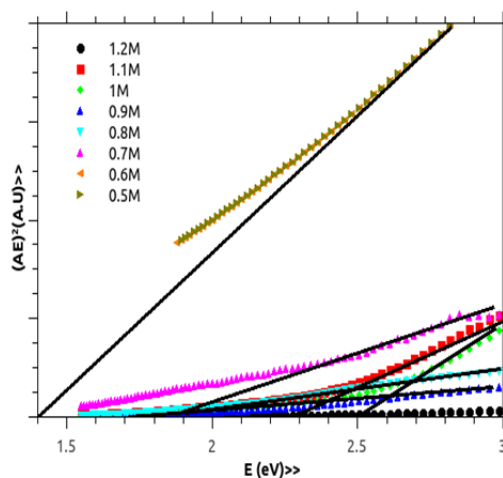


Fig. 3: Direct Band gap of the films

As expected, the band gap is the highest in 1.2M film and the least in 0.5M film. The variation of crystallite size and band gap at different molarities of $\text{Pb}(\text{CH}_3\text{COO})_2 \cdot 3\text{H}_2\text{O}$ is shown in the fig. 4. It establishes the inverse correlation between the two.

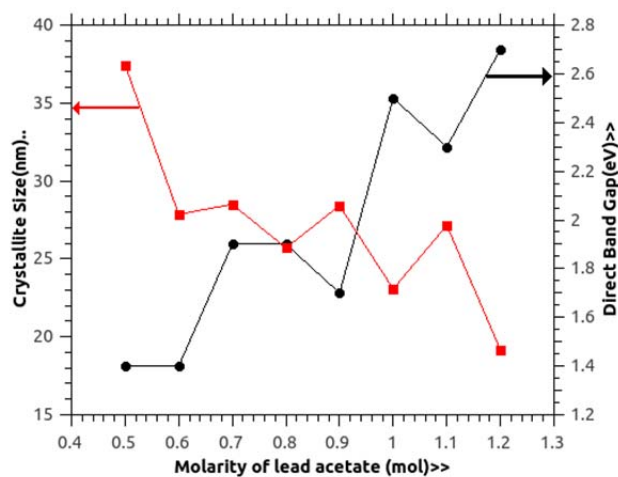


Fig. 4: Variation of crystallite size and band gap with molarities of lead acetate

The tails in the absorption spectrum signifying the electronic transitions among various mid gap states gives the Urbach energy[21] whose values are recorded in the Table 1.[Fig.5]. This energy is the least in the 0.5M film which is highly crystalline with least microstrain. The Urbach energies in the 0.6M and the 0.7M films are higher than those of the other films.

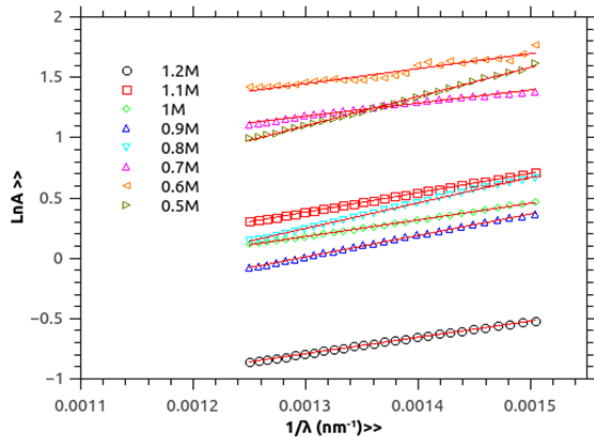


Fig. 5: Urbach Energy of the films deposited at various concentrations of lead acetate

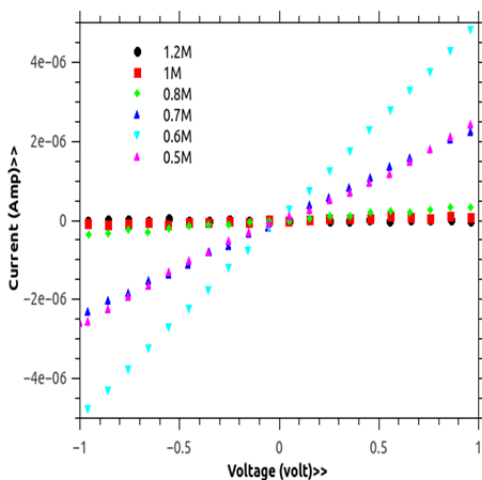


Fig. 6: Current-Voltage characteristics of the films.

3.3. Current-Voltage Characteristics of the Films

Fig. 6 shows the current-voltage characteristics of the films in the voltage range of -1 to +1 volt. It is observed that the current-voltage variations within the mentioned voltage range exhibits nearly Ohmic behaviour. The conductivities are estimated from the characteristics [22] and observed that it is higher $[(1.65-3.36) \times 10^{-3} (\Omega\text{cm})^{-1}]$ for 0.5M, 0.6M and 0.7M films, the 0.8M and 1.0M films have conductivities $\sim 10^{-4} (\Omega\text{cm})^{-1}$ and the 1.2M films have conductivity $\sim 6 \times 10^{-5} (\Omega\text{cm})^{-1}$. As we move from 0.5M to 1.2M, the strain increases with deteriorating crystallinity. The decrease in electrical conductivity can be indirectly related to the increase in strain in the films. Preetha et. al.[23] also reported similar observations.

4. CONCLUSION

We varied the concentration of lead acetate from 0.5 M to 1.2 M in a step of 0.1 M, keeping other parameters same. We observed that the film deposited from 0.5M lead acetate is highly crystalline with least strain and largest crystallites. The crystallinity deteriorates at higher concentrations of lead acetate and the crystallites become smaller. The effect of quantum size effect is prominently visible in all the films. The direct band gaps (1.4-2.7eV) are observed to be wider at higher molarities of lead acetate. The films deposited with lower concentration of lead acetate (0.5-0.7M) demonstrate better absorption property in the UV-Visible region. Also, as the concentration of lead acetate increases, the conductivity $(6 \times 10^{-5} - 1.88 \times 10^{-3}) (\Omega\text{cm})^{-1}$ decreases. It gets maximized in the film prepared from 0.6 M lead acetate. The film deposited from the bath containing 0.5 M lead acetate is of very good crystallinity with least strain, good absorption property, minimum density of mid gap states, good conduction characteristics and it observably exhibits quantum confinement of electrons and holes leading to remarkable blue shift of band gap (in comparison to the bulk PbS).

5. ACKNOWLEDGEMENT

The authors are grateful to SAIF, CUSAT for providing XRD and EDAX facility and the Department of Physics, Sibsagar College for UV-Visible spectrophotometer and Keithley Electrometer.

REFERENCES

- [1] Anna Osherov, Janos P Makai, Janos Balazs, Zsolt J Horvath, Nadav Gutman, Amir Sa'ar and Yuval Golan J. Phys.: Condens. Matter 22, doi:10.1088/0953-8984/22/26/262002 (2010)
- [2] J.D. Patel, T.K. Chaudhuri, Mater. Res. Bull. 44, 1647 (2009)
- [3] N. Choudhury, B.K. Sarma, Thin Solid Films 519, 2132 (2011)
- [4] P. Yang, C.F. Song, M.K. Lu, X. Yin, G.J. Zhou, D. Xu, D.R. Yuan, Chem. Phys. Lett. 345, 429 (2001)
- [5] H. Hirata, K. Higoshiyama, Bull. Chem. Soc. Jpn 44, 2420 (1971)
- [6] P.K. Nair, M.T.S. Nair, J. Phys. D Appl. Phys. 23, 150 (1990)
- [7] A. Martucci, J. Fick, J. Schell, G. Battaglin, M. Guglielmi, J. Appl. Phys. 86, 79 (1999)
- [8] H. Zhang, X. Ma, D Yang Materials Letters 58, 5 (2003)
- [9] T.L. Remadevi, K.C. Preetha, J. Mater. Sci. Mater. Electron. 23, 2017 (2012)
- [10] S. Jana, R. Thapa, R. Maity, K.K. Chattopadhyay, Phys. E 40, 3121 (2008)
- [11] J. Lee, Thin Solid Films 515, 6089 (2007)
- [12] S. Seghaier, N. Kamoun, R. Brini, A.B. Amara Materials Chemistry and Physics 97, 71 (2006)
- [13] N. Choudhury, B.K. Sarma, Indian J. Pure Appl. Phys. 46, 261 (2008)

-
- [14] S Zaman , S K Mehmood, M Mansoor, M M Asim IOP Conf. Series: Materials Science and Engineering 60 doi:10.1088/1757-899X/60/1/012057 (2014)
- [15] R. Thiagarajan, M. Mahaboob Beevi, M. Anusuya, T. Ramesh Optoelectronics And Advanced Materials – Rapid Communications 6, 132 (2012)
- [16] L. Beddek, M. Messaoudi, N. Attaf, M.S. Aida, J. Bougdira Journal of Alloys and Compounds 666, 327 (2016)
- [17] K. C. Preetha , T. L. Remadevi J Mater Sci: Mater Electron 24 489 (2013)
- [18] B.D. Cullity, S. R. Stock *Elements of X-Ray Diffraction* 2nd Impression (Pearson 2015) p.379
- [19] VD Mote, Y Purushotham and BN Dole *Journal of Theoretical and Applied Physics* 6:6 (2012)
- [20] K.C. Preetha, K.V. Murali, A.J. Ragina, K. Deepa, T.L. Remadevi Current Applied Physics 12, 53 (2012)
- [21] Ghobadi International Nano Letters 3:2 (2013)
- [22] A Goswami *Thin Film Fundamentals* [New Age International (P) Ltd.2008] p. 265
- [23] T. L. Remadevi, K. C. Preetha, , *J Mater Sci: Mater Electron* 23, 2017 (2012)